RAPID COMMUNICATIONS

PHYSICAL REVIEW C VOLUME 47, NUMBER 4 APRIL 1993

Antiproton production in $p + A$ collisions at 14.6 GeV/c

T. Abbott,[4,a] Y. Akiba,[7] D. Beavis,[2] M. A. Bloomer,[9,b] P. D. Bond,[2] C. Chasman,[2] Z. Chen,[2] Y. Y. Chu,[2] B. A. Cole,[9,c] J. B. Costales,[9,d] H. J. Crawford,[3] J. B. Cumming,[2] R. Debbe,[2] J. Engelage,[3] S.-Y. Fung,[4] S. Gushue,[2] H. Hamagaki,[7] O. Hansen,[2] R. Hayano,[10] S. Hayashi,[7,e] S. Homma,[7] H. Z. Huang,[9,b] Y. Ikeda,[8,f] I. Juricic,[5,g] J. Kang,[4] S. Katcoff,[2] S. Kaufman,[1] K. Kimura,[8] K. Kitamura,[6,h] K. Kurita,[5] R. J. Ledoux,[9,i] M. J. Le Vine,[2] Y. Miake,[2] R. J. Morse,[9] B. Moskowitz,[2] S. Nagamiya,[5] J. Olness,[2] C. G. Parsons,[9] L. P. Remsberg,[2] D. Roehrich,[2,j] H. Sakurai,[10] M. Sarabura,[9,k] P. Stankus,[5] S. G. Steadman,[9] G. S. F. Stephans,[9] T. Sugitate,[6] M. J. Tannenbaum,[2] J. H. Van Dijk,[2] F. Videbæk,[1,e] M. Vient,[4,l] P. Vincent,[2,m] V. Vutsadakis,[9] H. E. Wegner,[2] D. S. Woodruff,[9] Y. D. Wu,[5] and W. A. Zajc[5]

(E-802 Collaboration)

[1]*Physics Division, Argonne National Laboratory, Argonne, Illinois 60439*

[2]*Alternating Gradient Synchrotron, Chemistry and Physics Departments, Brookhaven National Laboratory, Upton, New York 11973*

[3]*Space Sciences Laboratory, University of California, Berkeley, California 94720*

[4]*University of California, Riverside, California 92507*

[5]*Columbia University, New York, New York 10027 and Nevis Laboratories, Irvington, New York 10533*

[6]*Department of Physics, Hiroshima University, Hiroshima 730, Japan*

[7]*Institute for Nuclear Study, University of Tokyo, Tanashi, Tokyo 188, Japan*

[8]*Kyushu University, Fukuoka 812, Japan*

[9]*Massachusetts Institute of Technology, Cambridge, Massachusetts 02139*

[10]*Department of Physics, University of Tokyo, Tokyo 113, Japan*

(Received 25 November 1992)

Antiproton production cross sections have been measured in minimum bias p+Be, p+Al, p+Cu, and p+Au collisions at 14.6 GeV/c with the E-802 spectrometer at the Brookhaven Alternating Gradient Synchrotron. The antiproton multiplicity at laboratory rapidities 1.0 to 1.6 shows almost no dependence upon the target mass. The $\bar{p}$ production for p+Be is somewhat lower than an estimation based upon 19–24 GeV/c $p+p$ data. In this rapidity interval the antiproton yield scales by a factor of 28±6 from p+Au to central Si+Au collisions.

PACS number(s): 25.75.+r

Experiment 802 at the Brookhaven Tandem Alternating Gradient Synchrotron (AGS) accelerator facility has measured semi-inclusive spectra of hadrons emitted from p, ^{16}O, and ^{28}Si induced reactions at 14.6A GeV/c with a variety of targets (Be, Al, Cu, and Au) (Refs. [1–4]). The antiproton production near midrapidity for Si+Al and Si+Au collisions [4] shows that the $\bar{p}$ multiplicity increases with target mass and centrality, but that the $\bar{p}/\pi^-$ ratio is smallest for central Si+Au collisions. In order to further elucidate the antiproton production in nuclear collisions and to attempt to understand the role of antiproton absorption, $\bar{p}$ yields in proton-nucleus collisions with various targets have been measured with the identical detector as in Ref. [4]. These measurements allow a direct comparison to the heavy ion results. The measurement of the target mass systematics is interesting, because hadronic formation times and absorption processes may result in a strong dependence of the antiproton yield on the target mass. The present results are for rapidities $y \leq y_{NN}$ and are compared in particular to previous results for $p + A$ and $p + p$ collisions [5] at 19.2 GeV/c. Antiproton production in the relativistic quantum molecular dynamics model has been discussed in Ref. [6]. The data presented here and in Ref. [4] are interpreted in a cascade model in the following paper by Kahana *et al.* [7].

The E-802 spectrometer [8] measures particle momenta for $p_t \geq 0.3$ GeV/c (p_t is the transverse momentum) and particle identification is provided by the time-of-flight system with a resolution of $\sigma \simeq 80$ ps. This allows a clean separation of $\bar{p}$ from K^- up to momenta of 3.7 GeV/c.

---

[a]Now at Reedley College, Reedley, CA 93654.

[b]Now at Lawrence Berkeley Laboratory, Berkeley, CA 94720.

[c]Present address: Columbia University, New York, NY 10027 and Nevis Laboratories, Irvington, NY 10533.

[d]Now at Lawrence Livermore National Laboratory, Livermore, CA 94550.

[e]Now at Brookhaven National Laboratory, Upton, NY 11973.

[f]Now at Hitachi Limited, Hitachi, Ibaraki 316, Japan.

[g]Now at Schlumberger Corp., Houston, TX 77210.

[h]Now at NTT Tsuyama, Tsuyama, Okayama 708, Japan.

[i]Now at Radionics Software Applications Corp., Brookline, MA 02146.

[j]On leave from University of Frankfurt, Fachbereich Physik, Frankfurt a.M., Germany.

[k]Now at Los Alamos National Laboratory, Los Alamos, NM 87545.

[l]Now at UC Irvine, Irvine, CA 92717.

[m]Now at Bruker Inc., Karlsruhe, Germany.

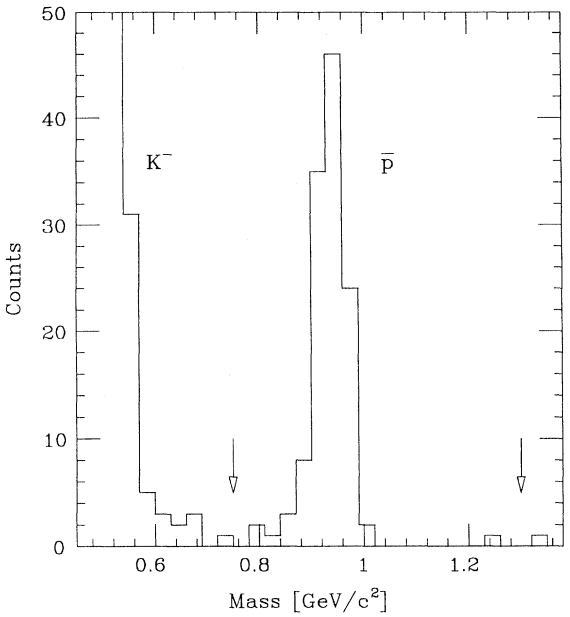

FIG. 1. Measured antiproton mass distribution summed over all targets within $1.0 \leq y \leq 1.6$ and $0.3 \leq p_t \leq 0.8$ GeV/c. The arrows indicate the mass cuts applied for antiproton separation. Note the zero suppression for the abscissa.

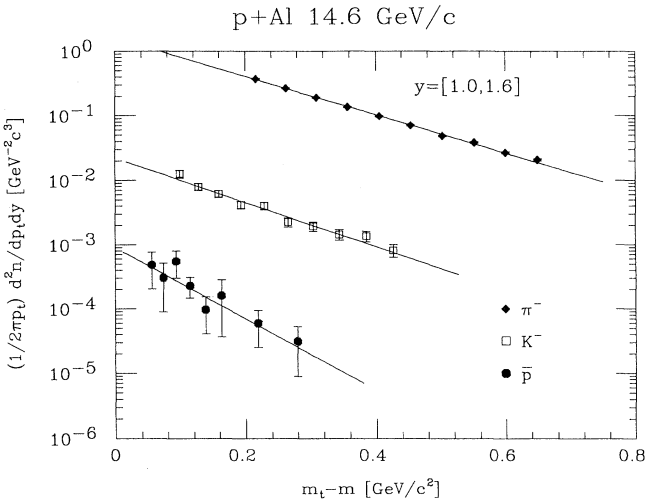

FIG. 2. Invariant spectra of negative pions, negative kaons, and antiprotons produced in $p+$Al collisions as a function of $m_t - m$, where $m_t \equiv (p_t^2 + m^2)^{1/2}$. Spectra have been normalized by using the inelastic cross sections quoted in Refs. [2,3], and plotted for a rapidity interval of $1.0 < y < 1.6$. Error bars reflect statistical uncertainties only. The systematic yield uncertainty is estimated to be $\pm 15\%$.

Since the nucleon-nucleon center-of-mass energy ($\sqrt{s} = 5.5$ GeV) of the experiment is just above the free nucleon-nucleon threshold ($\sqrt{s} = 3.8$ GeV) for $\bar{p}$ production, the cross section is small and the total number of detected antiprotons for all targets is only approximately 300. All the data are shown in Fig. 1. For each target these data have been corrected for background contamination ($\leq 5\%$), reconstruction efficiency (85%) and decay (where appropriate), target out contributions, and antiproton annihilation in the spectrometer (5%). An estimate of the systematic errors in overall normalization is $\sim 15\%$ for all targets. The corrections were made by the same method used in the $\bar{p}$ yields in Si$+A$ reactions reported by E-802 in Ref. [4] and are discussed in detail in Ref. [3]. In order to minimize possible biases at the edge of the acceptance, the analysis of the data was limited to a region in phase space (rapidity, y, and transverse momentum) with $1.0 \leq y \leq 1.6$ and $0.3 \leq p_t \leq 0.8$ GeV/c.

The differential invariant cross sections of negatively charged particles in $p+$Al collisions in the restricted y-p_t acceptance are shown in Fig. 2 plotted as a function of $m_t - m$ and normalized by using the inelastic cross section (see Ref. [3] for details). The $p+A$ minimum bias results are triggered by observing at least one charged particle in the spectrometer. The spectra of pions, kaons, and $\bar{p}$ in this wide rapidity interval ($\Delta y \simeq 0.6$) are well described by exponentials in transverse mass $(1/\sigma_{\text{inel}})(1/2\pi p_t) d^2\sigma/dp_t dy = A \exp[-(m_t - m)/B]$, where m is the rest mass, $m_t = (m^2 + p_t^2)^{1/2}$, and A and B (the inverse m_t slope) are the fit parameters. The resulting exponential fits to the spectra are indicated by solid lines. In previous analyses [1–4], a rapidity bin $\Delta y = 0.2$ has been used; the much wider bin here ($\Delta y = 0.6$) is necessary because of the low statistics of the $\bar{p}$. The corrections mentioned above, the wide y bin, and fluctuations due to the small number of counts may bias the data. Two methods, discussed below, for calculating dn/dy were therefore pursued.

First, if it is assumed that the invariant cross section for each type of particle can be characterized by a single exponential in m_t/B, the fraction of the cross section

TABLE I. Invariant cross section fraction and average p_t in the fiducial range as a function of the inverse slope B. The fiducial p_t range is $0.3 \leq p_t \leq 0.8$ GeV/c. The numbers are for an invariant cross section proportional to $\exp(-m_t/B)$ and do not represent any fit to data. See also the text for further explanation.

B	Cross section fraction			Apparent average p_t		
(MeV)	π^-	K^-	$\bar{p}$	π^-	K^-	$\bar{p}$
70	0.12	0.34	0.52	0.387	0.420	0.461
90	0.22	0.44	0.57	0.411	0.445	0.484
110	0.30	0.50	0.59	0.433	0.465	0.500
130	0.37	0.54	0.60	0.451	0.481	0.513
150	0.43	0.56	0.58	0.466	0.494	0.522
170	0.46	0.57	0.57	0.478	0.504	0.530

TABLE II. Multiplicity densities and particle ratios. Columns 2, 3, and 4 give dn/dy for π^-, K^-, and $\bar{p}$ production in the fiducial rapidity interval obtained from the average p_t procedure (see text). The two last columns quote the dn/dy ratios between $\bar{p}$ and π^- and $\bar{p}$ and K^- in the fiducial rapidity interval.

Collision system		$dn/dy\,(1.0 \le y \le 1.6)$ $10^1\pi^-$	10^2K^-	$10^4\bar{p}$	$10^3\bar{p}/\pi^-$	$\bar{p}/K^-$ (%)
$p+$Be	Min bias	3.89±0.03	0.92±0.05	3.8±0.8	1.0±0.2	4.2±0.8
$p+$Al	Min bias	4.40±0.03	1.17±0.05	4.7±1.0	1.1±0.2	4.0±0.9
$p+$Cu	Min bias	5.22±0.05	1.25±0.08	4.9±1.4	1.0±0.3	3.9±1.1
$p+$Au	Min bias	5.36±0.04	1.34±0.06	4.9±1.1	0.9±0.2	3.7±0.8

that falls in the fiducial p_t region ($0.3 \le p_t \le 0.8$ GeV/c) and the *average* p_t in the fiducial range may be calculated as a function of the inverse slope parameter B, as shown in Table I. The cross section fraction for antiprotons is rather insensitive to the slope. By comparison of the *average* p_t measured within the fiducial phase space with the calculated one, the inverse slope parameter B can be determined, leading to a determination of the fraction of the cross section in the chosen p_t range. These fractions (Table II) are ≈43% for pions, ≈54% for kaons, and ≈59% for antiprotons, essentially independent of target.

Second, an exponential was fitted to the invariant spectra ($\Delta y = 0.6$) as a function of $m_t - m$ and integrated to yield $dn/dy = 2\pi A(B^2 + mB)$. The stability of dn/dy and B as extracted from the fits was checked by varying the boundaries in y and p_t of the fiducial phase space and by applying two different fitting procedures (maximum likelihood for a Poisson distribution and the least-squares method). The results of the fits changed by less than 1σ when the fiducial window was moved by small amounts in the y-p_t plane, always keeping the window well within the acceptance. The dn/dy yields from the maximum likelihood method are higher (by $\approx 1\sigma$) than the ones from the least-squares fitting procedure. The yields determined by the $\langle p_t \rangle$ method as discussed above fall between the two fit results. dn/dy yields in the following therefore always refer to results obtained by the $\langle p_t \rangle$ method of determining B. It should be noted that summing over 0.6 unit of rapidity and fitting the integrated spectrum for the data presented here give the same result as fitting in narrow y bins of 0.1 and then averaging the dn/dy values. This latter consistency check was made for pions, where dn/dy is almost constant over the y acceptance, and, for protons, where dn/dy changes by a factor of 4 going from $y = 1.0$ to $y = 1.6$.

The dn/dy values from the $\langle p_t \rangle$ method are given in Table II. The inverse m_t slopes of the invariant spectra obtained by the two different fitting procedures and by the $\langle p_t \rangle$ method agree within their errors; the results for slopes discussed below are based on the least-squares fit. The inverse m_t slopes of the antiproton spectra for the various targets are similar and have a combined average of 93±18 MeV, which is smaller than those of K^- (129±5 MeV), π^- (147±1 MeV), and protons (130–160 MeV).

The inverse slopes of these antiproton spectra measured just below midrapidity are consistent with those obtained for $p+p$ (Ref. [5]) and smaller than those for

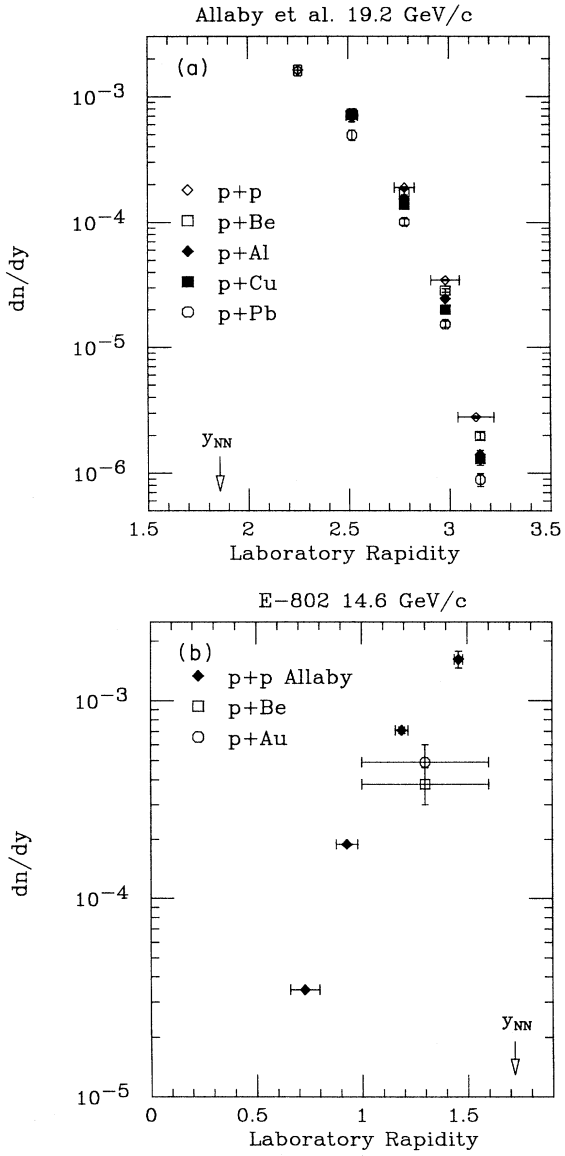

FIG. 3. (a) Antiproton dn/dy for $p+p$ and $p+A$ collisions [5] at 19.2 GeV/c. The arrow marked y_{NN} indicates the nucleon-nucleon center-of-mass rapidity for a 19.2 GeV/c proton beam on a fixed target. (b) dn/dy for antiprotons at 14.6 GeV/c (this experiment) for $p+$Be and $p+$Au. The filled diamonds are the 19.2 GeV/c $p+p$ results reflected about the 19.2 GeV/c y_{NN}. The y_{NN} arrow indicates the 14.6 GeV/c protons on fixed target nucleon-nucleon center-of-mass rapidity.

$p+A$ collisions [5,9] at higher beam energies (19–24 GeV/c). The antiproton invariant cross sections from Refs. [5,9] were replotted at fixed rapidity and are well represented by exponential distributions in m_t for transverse momenta down to the experimental cutoff of 50 MeV/c. From the distributions at higher energies inverse m_t slopes are extracted of 110–130 MeV for $p+p$ collisions and 130–170 MeV for $p+A$ collisions, albeit at rapidities greater than y_{NN}. Compared to the antiproton inverse m_t slopes in central Si+Al and central Si+Au collisions [4] of 141±14 MeV, the corresponding values for proton induced reactions are significantly smaller. The inverse slopes from p+Be, Al, Cu, and Ta, measured by Boyarinov *et al.* [10] at an incident momentum of 10.1 GeV/c and $y \approx 0$ range from 65 MeV (Be) to 82 MeV (Ta), slightly below the present values.

Rapidity density distributions were extracted from $p+p$ and $p+A$ data at higher energies, assuming that the invariant cross sections at fixed rapidity are described by exponentials (see, e.g., Ref. [11]). The rapidity density distribution inferred from the data of Allaby *et al.* (Ref. [5]) is shown in Fig. 3(a). The yields of antiprotons from $p+p$ and $p+A$ collisions are similar in the rapidity interval just above y_{NN}. Also shown are the yields obtained in this experiment for Be and Au [Fig. 3(b)]. They are about a factor of 2 lower than the $p+p$ data at 19.2 GeV/c reflected about y_{NN} [see Fig. 3(b)]. This is due to the strong $\sqrt{s}$ dependence of the antiproton production cross section and is in rough agreement with an extrapolation of the $\sqrt{s}$ trend in the $p+p$ data [12,13]. The $p+p$ rapidity density distributions are centered at y_{NN} and have a FWHM of $\simeq 1.2$ units of rapidity.

The 10.1 GeV/c dn/dy values [10] for Al, Cu, and Ta at $y \approx 0$ are nearly target independent and about a factor of 100 smaller than values in Table II, while the p+Be result is yet another factor of 2 smaller.

Total multiplicities have been measured [14] at 24 GeV/c for $p+p$ collisions leading to $\bar{p}$, K^-, and $\pi^\pm$. Based on the $\sqrt{s}$ systematics of Ref. [13] these results can be extrapolated to 14.6 GeV/c. The ratios $2\bar{p}/(\pi^+ + \pi^-)$ and $\bar{p}/K^-$ are estimated in this way as $(1.0\pm0.1)\times10^{-3}$ and $(6.7\pm0.8)\times10^{-2}$, respectively. At 14.6 GeV/c the π^+ and π^- yields for p+Be are similar in the fiducial rapidity range considered here (see Ref. [3]), so the $\bar{p}/\pi^-$ result in Table II also represents $2\bar{p}/(\pi^+ + \pi^-)$ and is equal to the $p+p$ extrapolated full phase space result; the p+Be $\bar{p}/K^-$ ratio $(4.2\pm0.8)\times10^{-2}$ is smaller than the $p+p$ result. The $\bar{p}$ multiplicity from the 24 GeV/c data extrapolated to 14.6 GeV/c is $(1.2\pm0.1)\times10^{-3}$, where the uncertainty does not include the extrapolation.

The $\bar{p}/\pi^-$ and the $\bar{p}/K^-$ ratios for various targets (Table II) show no target dependence, and are about 0.1% and about 4%, respectively. The $\bar{p}/\pi^-$ ratio for central Si+Al and Si+Au collisions [4] within the errors agrees with the ratio for $p+A$ collisions, while the $\bar{p}/K^-$ ratio in central Si+Au collisions is smaller than for p+Au.

Table III shows the ratio of $\bar{p}$, K^-, and π^- yields in the same phase space window from central Si+A collisions relative to those from the corresponding minimum bias $p+A$ collisions. In this table the Si+A central collision yields were obtained with a trigger set on the upper 7% of the charged particle multiplicity. The (Si+Au)/(p+Au) ratio is approximately 28 for both pion and antiproton production while the (Si+Al)/(p+Al) $\bar{p}$ and π^- ratios are close to 20; both $\bar{p}$ ratios have large uncertainties. The corresponding K^- ratios are larger by $\approx 50\%$.

TABLE III. Ratios of particles produced in minimum bias $p+A$ and in central Si+A collisions at 14.6A GeV/c. The $p+A$ data are from the present experiment while the Si+A results are from Ref. [4]. (See also the text.)

	Ratio $(1.0 \le y \le 1.6)$		
Collision system	π^-	K^-	$\bar{p}$
(Si+Al)/(p+Al)	18±1	28±7	21±6
(Si+Au)/(p+Au)	31±1	47±6	28±6

In a black nucleus approach one may assume that the antiproton production cross section shows an $A^{2/3}$ dependence, while the average absorption path of the $\bar{p}$ varies as $A^{1/3}$, resulting in an overall target mass dependence of the multiplicity $\propto \exp(-\chi A^{1/3})$ where χ is proportional to the inverse mean free path of the antiproton. The rapidity densities are shown as a function of target A in Fig. 4. The dn/dy of antiprotons is not very dependent on the target mass; the data at higher energies above midrapidity show a small decrease with A (less than $\simeq 30\%$) (see also Ref. [15]), while our data below midrapidity indicate that the antiproton yield is constant or increases slightly with target mass ($\simeq 30\%$, within 1σ). Because of the very large annihilation cross section this lack of a strong A dependence is surprising and is consistent with a black nucleus for the production and considerably reduced absorption for the outgoing $\bar{p}$. A theoretical explanation for this is provided in the following paper [7]. The target mass systematics presented earlier for π^- and K^- are very similar.

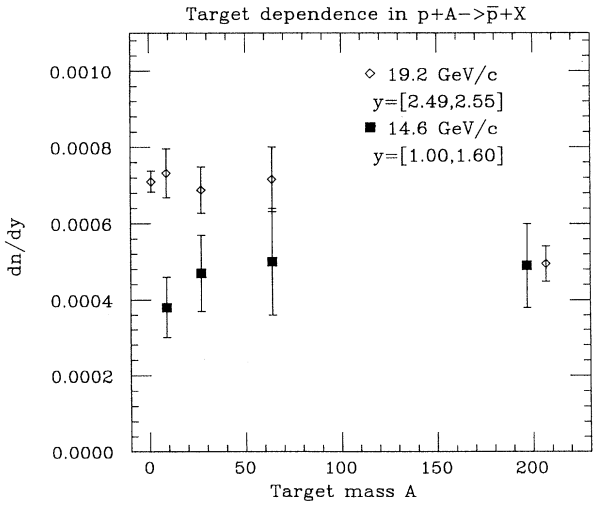

FIG. 4. Target mass dependence of the rapidity density of antiprotons produced in minimum bias $p+A$ collisions at 14.6 GeV/c and in $p+p$ and $p+A$ collisions [5] at 19.2 GeV/c. The errors shown are only statistical.

Table III shows that the central collision Si+Au$\rightarrow\bar{p}+X$ multiplicity is 28 ± 6 times the $p+$Au$\rightarrow\bar{p}+X$ multiplicity in the rapidity range $1.0\leq y\leq 1.6$. In Ref. [4], the Si+Au result was compared to a first strike model, i.e., a model in which antiprotons are only created in interactions between a projectile nucleon and a target nucleon neither of which have been previously struck. The FRITIOF model [16] showed that a central Si+Au collision on the average has 13 such first strike interactions. Using the extrapolated $p+p$ result, quoted above, the Si+Au measurement was $\simeq 1.4$ times the prediction of the first strike estimate. If we take the measured $p+$Au multiplicity density (Table II) as a template, the Si+Au result is 28 times larger, i.e., twice the first strike value. This is consistent with the fact that the $p+$Au value in Table II is 1.35 times smaller than the $p+p$ value used in Ref. [4], when the latter is cut into the presently used rapidity interval (see, in particular, Fig. 3 of Ref. [4]). The Si+Au value (Table III) is also roughly twice the first strike value, if the presently measured $p+$Al result is used as a template. If $p+$Be is used, the factor is ≈ 2.5 times the first strike number.

In summary, we report on the measurements of antiproton production in $p+A$ collisions at 14.6 GeV/c. The antiproton yield below y_{NN} shows almost no target mass dependence, the relative yields compared to π^- and K^- stay constant. The antiproton yields in going from $p+A$ to central Si+A collisions are consistent with a scaling with the number of participating projectile nucleons.

This work has been supported by the U.S. Department of Energy contracts with ANL (W-31-109-ENG-38), BNL (DE-AC02-76CH00016), Columbia University (DE-FG02-86-ER40281), MIT (DE-AC02-76ER03069), University of California, Riverside (DE-FG03-86ER40271), and by NASA (NGR-05-003-513), under contract with the University of California, and by the U.S.-Japan High Energy Physics Collaboration Treaty.

[1] E-802 Collaboration, T. Abbott *et al.*, Phys. Rev. Lett. **64**, 847 (1990).
[2] E-802 Collaboration, T. Abbott *et al.*, Phys. Rev. Lett. **66**, 1567 (1991).
[3] E-802 Collaboration, T. Abbott *et al.*, Phys. Rev. D **45**, 3906 (1992).
[4] E-802 Collaboration, T. Abbott *et al.*, Phys. Lett. B **271**, 447 (1991).
[5] J. V. Allaby *et al.*, CERN Report No. 70-12, 1970 (unpublished).
[6] A. Jahns, H. Stöcker, W. Greiner, and H. Sorge, Phys. Rev. Lett. **68**, 2895 (1992).
[7] S. Kahana, Y. Pang, T. J. Schlagel, and C. Dover, Phys. Rev. C **47**, R1356 (1993), the following paper.
[8] E-802 Collaboration, T. Abbott *et al.*, Nucl. Instrum. Methods **A290**, 41 (1990), and references therein.
[9] T. Eichten *et al.*, Nucl. Phys. **B44**, 333 (1972).
[10] S. V. Boyarinov *et al.*, Yad. Fiz. **54**, 119 (1991) [Sov. J. Nucl. Phys. **54**, 71 (1991)].
[11] J. B. Costales, Ph.D. thesis, MIT, 1990.
[12] A. M. Rossi *et al.*, Nucl. Phys. **B84**, 269 (1975).
[13] A. Wroblewski, in Proceedings of the International Symposium on Multiparticle Dynamics, Kayserberg, 1977 (unpublished), p. A1; Acta Phys. Pol. **B15**, 785 (1984).
[14] U. Amaldi *et al.*, Nucl. Phys. **B86**, 403 (1975).
[15] D. Dekkers *et al.*, Phys. Rev. **137**, B962 (1965); L. M. Barkov *et al.*, Z. Phys. C **14**, 1 (1982).
[16] B. Nilsson-Almqvist and E. Stenlund, Comput. Phys. Commun. **43**, 387 (1987).